Clinical Radiology 74 (2019) 663–675

Contents lists available at ScienceDirect

Clinical Radiology

journal homepage: www.clinicalradiologyonline.net

Pictorial Review

Subdural haematoma mimics

M. Lim [a,*], S.W. Kheok [a], K.C. Lim [a], N. Venkatanarasimha [a], J.E. Small [b], R.C. Chen [a]

[a] Department of Diagnostic Radiology, Singapore General Hospital, Singapore
[b] Neuroradiology, Lahey Hospital and Medical Center, Burlington, MA, USA

ARTICLE INFORMATION

Article history:
Received 26 October 2018
Accepted 9 April 2019

A subdural haematoma (SDH) is a frequently encountered pathology seen on an emergency room computed tomography (CT) head scan. An extra-axial crescentic density along the convexity of the brain or within the interhemispheric fissure is generally thought to represent a SDH; however, SDH mimics are known to occur in nature, and can be broadly classified under the subcategories of normal anatomy, artefacts, tumour, inflammation, infection, ischaemia, trauma, and iatrogenic. Understanding the typical characteristics of a SDH, knowledge of normal anatomy, close inspection of the morphology of the subdural process, changes to the adjacent structures, and rigorous attention to clinical details may reveal subtle clues that distinguish a true SDH from a mimic. This is crucial in appropriately directing clinical management. This review amalgamates most of the rare subdural processes that have been reported to mimic SDH, and discusses the imaging and clinical features that help to differentiate between them. This topic is highly valuable for radiology trainees, general radiologists, and emergency room physicians, and may serve as a refresher for the practising neuroradiologist.

Introduction

A subdural haematoma (SDH) is a common entity encountered on an emergency room computed tomography (CT) scan; however, there are many mimics of SDH and it may be challenging to distinguish these from a true SDH. Understanding the typical characteristics of a SDH, knowledge of normal anatomy, close inspection of the morphology and neighbouring structures of the subdural process, and rigorous attention to the clinical details may reveal subtle clues that distinguish the two, as the correct diagnosis is essential in the subsequent management of these patients.[1] This review will outline some of the commonly encountered SDH mimics, which can be categorised into the following groups: normal anatomy, artefacts, tumour, inflammation/infection, ischaemic and trauma/iatrogenic (Table 1).

Subdural haematoma

A SDH is a misnomer, as it actually refers to a collection of extra-axial blood accumulating in the inner most layer of the dura, termed the border cell layer (Fig 1). A true subdural space does not exist. The border cell layer is a region of structural weakness in which blood can accumulate within and dissect along.[2] SDHs are usually traumatic in nature and result from the stretching and tearing of cortical veins linking the cerebral cortex and the dural sinuses.[3]

* Guarantor and correspondent: M. Lim, Department of Diagnostic Radiology, Singapore General Hospital, Outram Road, Singapore 169608, Singapore. Tel.: +65 6222 3322.
E-mail address: may.lim@mohh.com.sg (M. Lim).

https://doi.org/10.1016/j.crad.2019.04.013
0009-9260/

Table 1
Differentials for dural based lesions that mimic subdural haematomas.

Mimicker subgroup	Pathology
Normal anatomy and artefacts	Sphenoparietal sinus
	Prominent transverse sinus
	Frontal lobe extending into the middle cranial fossa
	Cerebellar flocculus
	Beam-hardening artefact
	Motion artefact
Tumours	Lymphoma
	Metastases
	Granulocytic sarcoma
	Meningioma
	Solitary fibrous tumour
Ischaemic	Hypoxic ischaemic injury
Infection/inflammatory	Hypertrophic pachymeningitis
	Empyema
	Rosai–Dorfman disease
Traumatic/iatrogenic	Epidural haematoma
	Subdural hygroma
	Intracranial hypotension
	Post-shunt meningeal fibrosis

On axial imaging, a SDH classically appears as a smoothly marginated crescent-shaped extra-axial collection overlying the cerebral convexities (Fig 2a,b).[4] SDHs demonstrate marked heterogeneity in appearance on imaging due to differing proportions and mixtures of clotted blood, unclotted blood, and bloody and clear cerebrospinal fluid (CSF).[2] The appearance of SDHs on unenhanced CT and magnetic resonance imaging (MRI) further varies with evolution of the haematoma (Fig 2c,d). This differs from that of intra-parenchymal haematomas due to the lack of a blood–brain barrier in the subdural space, thereby resulting in differing rates of haemosiderin clearance into the chronic phase.[5] These imaging features are summarised in Table 2. A SDH should not show central post-contrast enhancement on either CT or MRI.

SDHs may cross calvarial sutures but rarely cross the midline, typically residing in the supratentorial region along the cerebral convexity. They can also extend along either the falx cerebri and/or tentorium cerebelli.[6,7] In a study of 309 patients, 93% SDHs occurred in the parietal region, 88% in the frontal region, and 34% in the occipital region.[8] SDHs can, yet less commonly, extend inferiorly past the level of the Sylvian fissure.[7] They rarely occur in the posterior cranial fossa adjacent to the cerebellar hemispheres.[9]

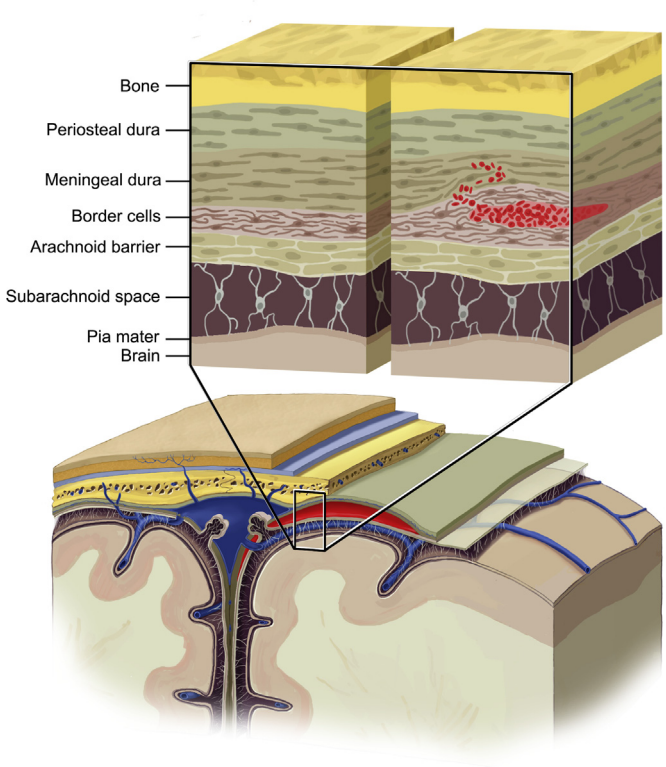

Figure 1 Schematic diagram demonstrating the brain and its coverings. A SDH occurs in the inner most layer of the dura, termed the border cell layer. A true subdural space does not exist.

Normal anatomy and artefacts mimicking subdural haematoma

Normal anatomical structures can be potentially mistaken for SDHs when there is lack of familiarity with the varied appearances of normal venous and lobar anatomy.

Prominent venous sinuses

A prominent and slightly hyperdense transverse venous sinus may be mistaken for a SDH along the tentorial leaflets (Fig 3a). These sinuses can be particularly pronounced when haematocrit levels are raised.[10] Prominent sphenoparietal sinuses may also be mistaken for acute SDH along the anterior aspect of the middle cranial fossae (Fig 3b,c). These normal structures can be quite engorged, yet understanding that a normal venous sinus lies in this region will aid in avoiding this pitfall. Furthermore, when SDHs occur in the middle cranial fossa, they are typically along the lateral border of the temporal lobe, rather than along its anterior rim. If further confusion persists, a contrast-enhanced examination showing homogeneous central enhancement will confidently distinguish these normal venous sinuses from SDHs.

Prominent cortical veins

Prominent cortical veins may mimic slivers of SDH when seen on isolated sections of a CT head images. On orthogonal projections, these structures will demonstrate the tubular, tortuous nature of the vessel, and their communication with the dural venous sinuses (Fig 3d,e).[11]

Frontal lobes and cerebellar flocculus

Frontal lobes extending posteriorly into the middle cranial fossa may occasionally appear to be an “extra-

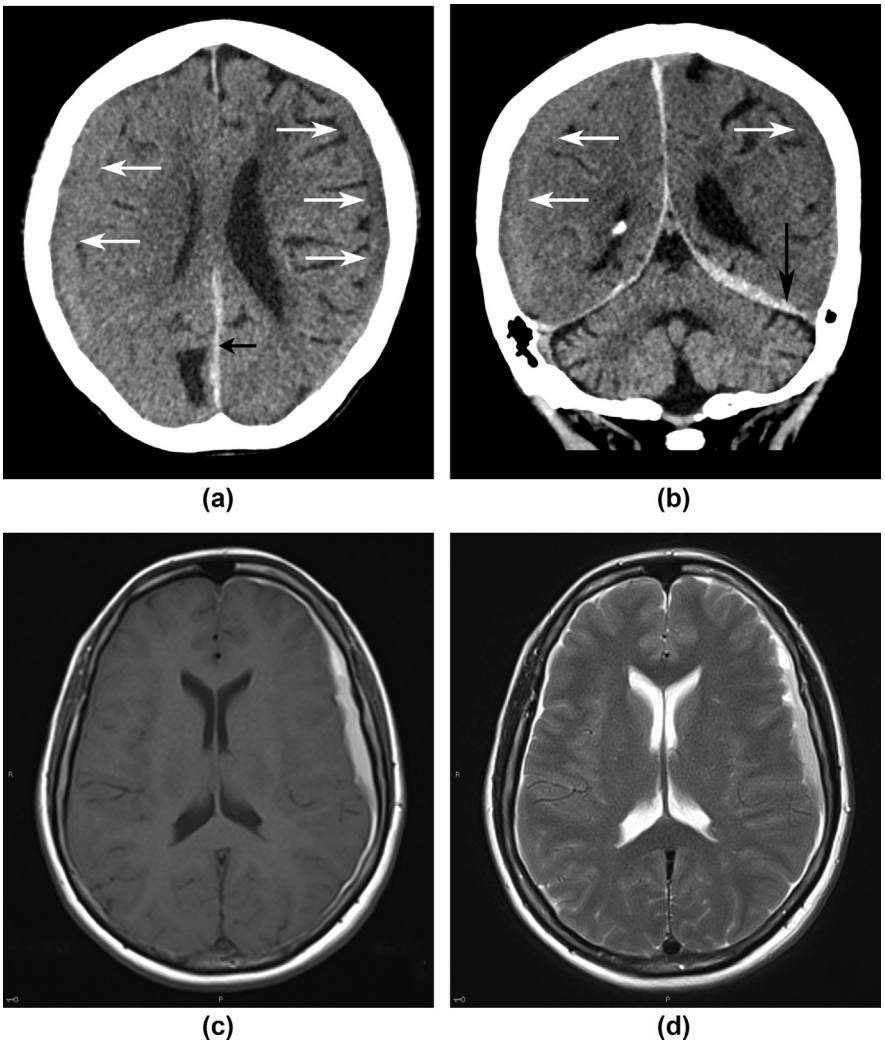

Figure 2 Appearance of SDHs on CT and MRI. Patient 1: a 71-year-old woman presenting after a fall with head injury. (a,b) Unenhanced axial and coronal CT head images demonstrate SDHs of varying ages over the cerebral convexities (white arrows), interhemispheric fissure (short black arrow) and tentorial leaflet (long black arrow). Note the smooth crescentic shape of the SDHs, which cross suture lines. Patient 2: a 55-year-old woman had a MRI head performed for investigation of headache. (c,d) Axial T1-weighted and T2-weighted images showing high T1 and mixed T2 signal, compatible with a mixed early to late subacute SDH overlying the left cerebral convexity.

Table 2
Typical imaging appearances of a subdural haematoma (SDH) at different stages of evolution on computed tomography (CT) and magnetic resonance imaging (MRI).

Chronicity of bleed	CT[6]	MRI[a,5,63]	
		T1-weighted images	T2-weighted images
Hyperacute (24 h)	Hyperdense (60–80 HU; decrease 1.5 HU per day)	Low signal/isointense	High signal
Acute (24–48 h)		Low signal/isointense	Low signal
Subacute (2–7 days)	Varying density; remains mostly hypodense relative to grey matter	High signal	Low signal
Late subacute (7–14 days)		High signal	High signal
Chronic (>21 days)	Hypodense relative to grey matter	Low signal/isointense	High signal

[a] The signal intensity of SDHs on MRI as described in this table is relative to grey matter. Note also that the appearance of evolving SDH on MRI differs from that of intra-parenchymal haematomas due to various factors, including the lack of a blood–brain barrier in the subdural space resulting in differing rates of haemosiderin clearance in the chronic phase, and tendency to rebleed.[5] Note that varying mixtures of CSF, clotted blood, and unclotted blood may be present within a SDH at any point in time.[2]

axial lesion" (Fig 3f). Likewise, the nodular appearance of the cerebellar flocculus as it protrudes off of the main body of the cerebellum can be mistaken for an extra-axial process (Fig 3g).[12] Careful inspection showing the presence of grey–white matter differentiation within the "lesion" will aid in avoiding this pitfall.

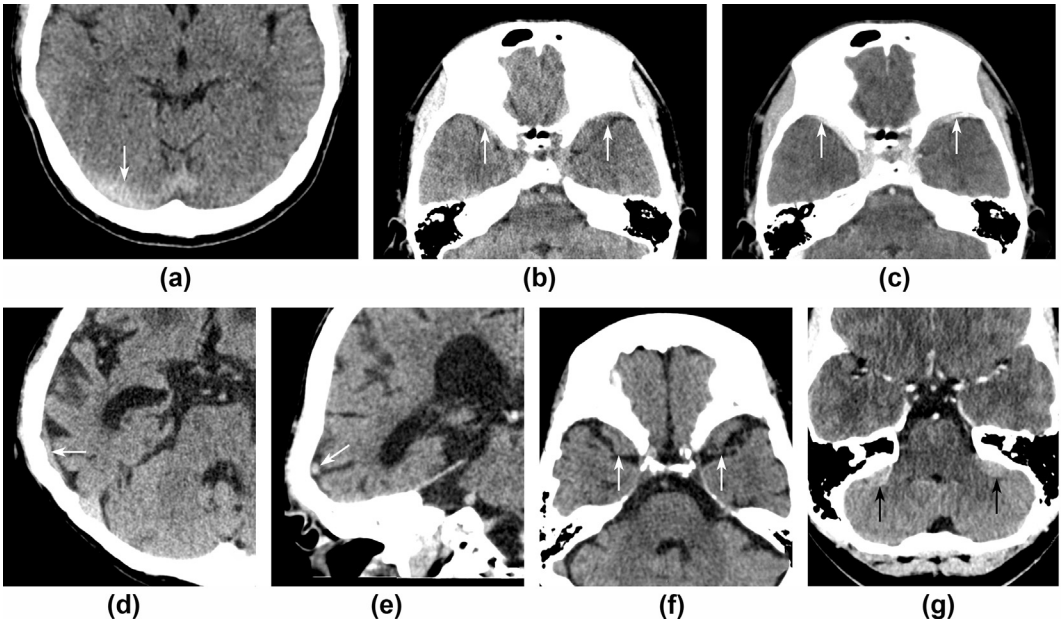

Figure 3 Normal anatomy that mimics SDH. Patient 1: a 49-year-old man presenting with vertiginous giddiness. (a) Unenhanced axial CT brain image demonstrates a prominent right transverse sinus, which mimics the appearance of a SDH (white arrow). His haematocrit value was raised at 57.8% (normal range 38–52%). Patient 2: a 20-year-old man presenting with headache for three months. (b) Unenhanced axial CT head image shows extra-axial crescentic densities along the anterior aspect of the middle cranial fossa (white arrows). (c) Homogeneous enhancement is noted on the post-contrast enhanced images (white arrows). This is a typical location for the sphenoparietal venous sinus, which should not be confused for a SDH. Patient 3: a 75-year-old man had a CT head scan performed after sustaining a head injury. (d) Unenhanced axial CT head image demonstrates an extra-axial hyperdensity within the right temporal fossa, which appears to be an acute SDH (white arrow). (e) The orthogonal coronal projection shows this lesion corresponds to a prominent cortical vein (white arrow). Patient 4: an 86-year-old woman presenting with head injury after a fall. (f) Unenhanced axial CT head image shows the frontal lobes extending posteriorly into the middle cranial fossa bilaterally (white arrows). The presence of grey and white matter differentiation within the "lesion" can be confidently attributed to normal brain cortex. Patient 5: an 18-year-old presenting with new-onset headache. (g) Axial CT head image shows the cerebellar flocculus along the petrous face of the temporal bones (white arrows). Familiarity with normal anatomy will avoid mistaking this for an extra-axial process.

Artefacts

Beam-hardening occurs when lower-energy photons in an X-ray beam during CT are absorbed more rapidly than the higher-energy photons as they pass through an object.[13] This can result in streak artefacts along the inner surface of the bony calvarium, which may mimic SDH, especially along the anterior cranial fossa (Fig 4a).[13] Beam-hardening may be minimised by using filtration, calibration correction, and beam-hardening correction software. Patient motion can cause misregistration artefacts, which usually appear as shading or streaking in the reconstructed image, which may also mimic SDH (Fig 4b).[13]

Tumours

Lack of a clear trauma history, persistence or growth on follow-up imaging, and a nodular appearance of the subdural process may be red flags that a dural tumour may be present. If uncertainty persists, a contrast-enhanced examination or MRI may clinch the diagnosis.[14,15]

Lymphoma

Central nervous system (CNS) lymphomas consist of two major subtypes: primary CNS lymphomas and secondary CNS lymphoma from a systemic source. Lymphomas that mimic SDH tend to be primary lymphomas arising from the dura.[1] Primary dural lymphomas make up <1% of all CNS lymphomas with mucosal associated lymphoid tissue (MALT) lymphomas being the most common; the remainder are high-grade diffuse large B-cell lymphomas.[16,17]

Secondary lymphomas are overall more common than primary CNS lymphomas. Secondary dural lymphomas occur by direct spread from the bones of the skull, or in continuity with meningeal deposits that spread via the cranial nerves.[18] Approximately two-thirds of patients show leptomeningeal involvement, and one-third have parenchymal disease.[19]

Similar to SDH, CNS lymphomas are hyperattenuating on CT (Fig 5a).[16] On MRI, they are isointense to hypointense on T2-weighted images and demonstrate restricted diffusion due to dense cell packing. Central enhancement on post-contrast images and vasogenic oedema is frequently seen (Fig 5b,c).[16] The associated leptomeningeal enhancement may be more apparent on MRI.[18]

Metastases

Dural metastases result from contiguous extension of adjacent skull metastasis or via direct haematogenous

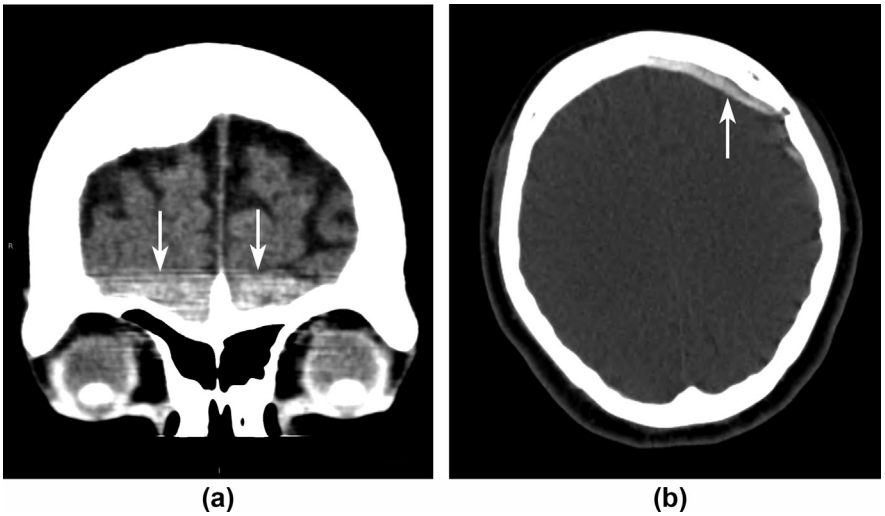

Figure 4 Artefacts that mimic SDH. Patient 1: a 62-year-old woman had a CT head scan done to follow-up on a subarachnoid haemorrhage. (a) Unenhanced coronal CT head image demonstrates beam-hardening artefact mimicking a subdural haemorrhage along the frontal convexities (white arrow). Patient 2: a 49-year-old woman presenting with head injury. (b) Unenhanced axial CT head image demonstrates motion artefact mimicking a subdural haemorrhage along the frontal convexity (white arrow). Blurring of the bone and brain parenchyma will help in diagnosing motion artefact.

spread to the dural vasculature. They most commonly arise from a primary prostate malignancy (19.5%), followed by breast (16.5%), lung (11%), and stomach malignancies (7.5%).[20] Melanoma, renal cell carcinoma, and gastric carcinoma also have been known to cause dural metastases, albeit rarely.[16]

Dural metastases with superimposed SDH have also been known to occur in 15–40% of cases, either secondary to rupture of tumour vessels or rupture of dural vessels from increased intracranial pressure.[20] Dural metastases are frequently solitary and may present as linear dural thickening, nodular lesions or as an extensive en plaque subdural tumour (Fig 5d).[16,21,22] Vivid enhancement on post-contrast images is often seen. In contrast to simple SDHs, adjacent bony involvement may be present. The nodular margins of the tumour may be more apparent on MRI (Fig 5e,f). Similar to meningiomas, dural metastases may have an enhancing dural tail.[16,18]

Meningioma

A meningioma is the most common intracranial neoplasm and most common extra-axial mass, accounting for 30% of adult intracranial neoplasms. They are non-glial neoplasms that originate from the meningocytes or arachnoid cap cells of the meninges.[23,24] Meningiomas may manifest as expansile extra-axial masses with a wide dural attachment, or as en plaque dural tumour. They commonly occur along the falx, parafalcine region, cerebello-pontine angle, and planum sphenoidale.[23]

CT demonstrates roughly 60% of meningiomas to be hyperdense (Fig 5g), while 20% demonstrate calcification. Adjacent bony changes such as hyperostosis and osteolysis have been reported in up to 40% of cases, distinguishing them from SDHs.[24] A rare meningioma subtype, the intraosseous meningioma, may cause sclerotic expansion of the inner and outer tables of the calvarium.[23]

The vast majority will demonstrate intense homogeneous post-contrast enhancement (Fig 5h,i), and can be associated with peri-lesional vasogenic oedema.[23,24] A meningioma can show a “cleft sign”, whereby CSF, hypointense dura or marginal blood vessels are trapped between the lesion and the underlying brain parenchyma.[24] Furthermore, enhancement of the dura trailing off away from the lesion in a crescentic fashion (dural tail) can typically be seen on MRI.[23]

Granulocytic sarcoma

Granulocytic sarcomas, also known as chloromas, are rare extramedullary tumours comprised of leukaemia myeloid precursors, occurring most commonly in patients with acute myelogenous leukaemia (46.3%).[25,26] They can also be seen in patients with chronic myelogenous leukaemia or other myeloproliferative diseases such as myelofibrosis with myeloid metaplasia, hypereosinophilic syndrome, or polycythaemia vera.[27] A chloroma will develop in 2.5–9.1% of patients with acute myelogenous leukaemia, which is five-times more frequent than chronic myelogenous leukaemia patients.[28] These solid tumours of myeloid lineage were initially termed chloromas because of their greenish hue from their inherent myeloperoxidase enzyme. Most occur in patients <15 years of age, and their presence is important as they can portend an impending blast crisis.[29] Potential sites of involvement include the CNS, bone, subcutaneous tissues, genitourinary system, lymph nodes, orbits, and skin.[25,27] In the CNS, they are thought to arise from dural and subarachnoid veins and surrounding adventitia, and are contiguous with the meninges or

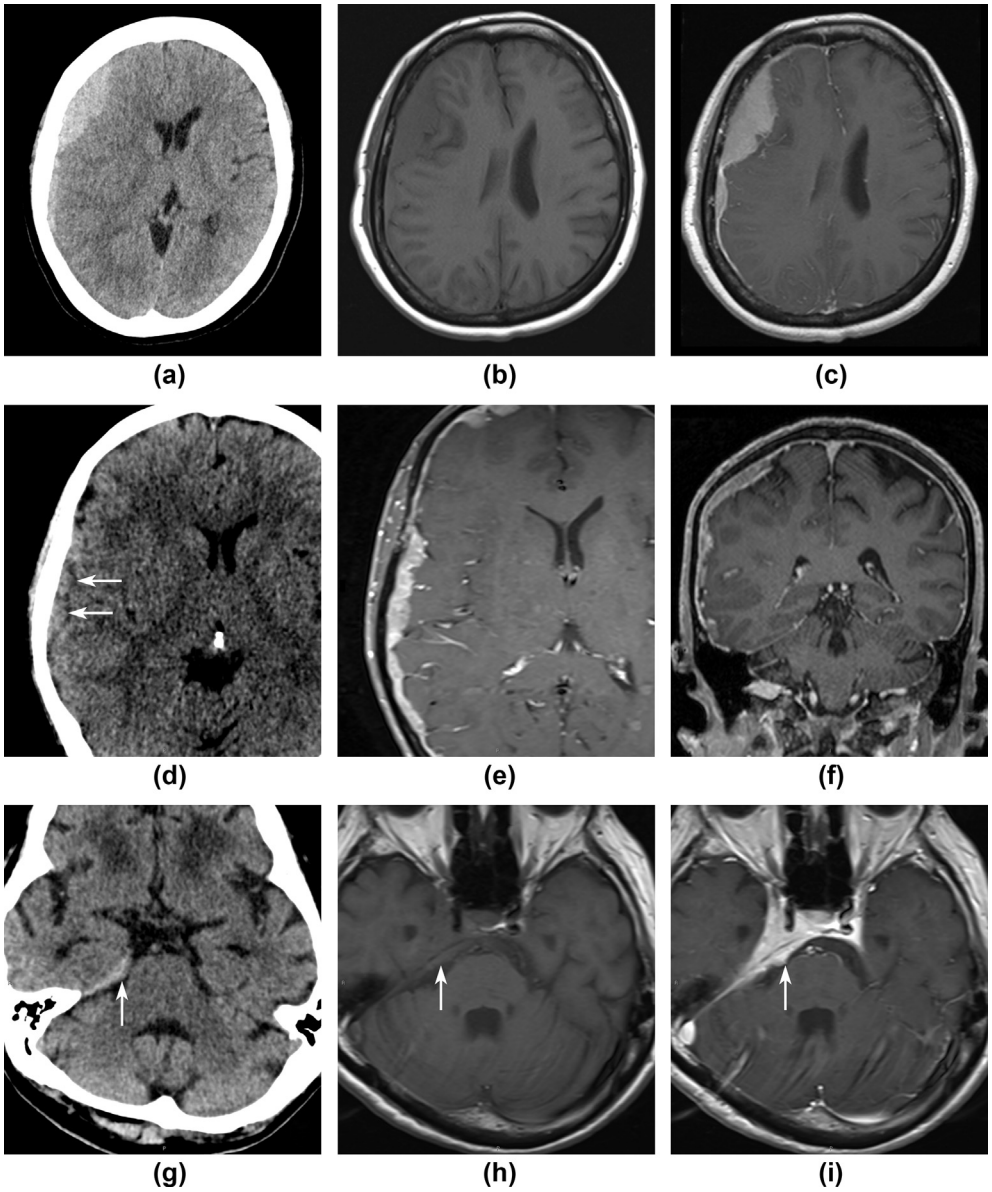

Figure 5 Tumours that mimic SDHs. Patient 1: a 55-year-old woman presenting with headache. (a) Unenhanced axial CT head image demonstrates a lobulate hyperdense extra-axial lesion along the right cerebral convexity, which was initially interpreted as a SDH. (b,c) Pre- and post-contrast T1-weighted axial MRI images show that the lesion demonstrates vivid homogeneous post-contrast enhancement. The patient underwent a biopsy of the lesion, and the final histological diagnosis was that of extra-nodal marginal zone B-cell lymphoma with florid reactive plasmacytosis. Patient 2: a 61-year-old man with a history of metastatic prostate carcinoma presenting with slurred speech and facial asymmetry. (d) Unenhanced CT head axial image demonstrates a crescent-shaped isodense extra-axial lesion along the right cerebral convexity which appears to be a SDH (white arrows). (e,f) On the post-contrast T1-weighted axial and coronal MRI images, this lesion is noted to demonstrate vivid post-contrast enhancement. Note that the lesion now clearly demonstrates lobulate borders, which is not well seen on CT. The findings represent dural metastasis along the right cerebral convexity. Patient 3: a 72-year-old woman presenting with an unwitnessed fall and left lower-limb weakness. (g) Unenhanced axial CT head demonstrates hyperdense thickening of the right tentorial leaflet, suggestive of a SDH (white arrow). (h,i) Pre- and post-contrast T1-weighted axial MRI images show diffuse enhancement of this process with associated dural tail (white arrows). The findings represent a meningioma along the right tentorial leaflet with contiguous extension into the cavernous sinus.

ependyma.[28] Prognosis is dismal, with median survival rates of 7.5 months.[29]

CNS granulocytic sarcomas more often occur along the meninges than within the brain parenchyma. When seen on CT, they are usually hyperdense to brain parenchyma, and on MRI, they are hypointense or isointense on T1-weighted images, and heterogeneously isointense or hyperintense on T2-weighted images.[27,28] Homogeneous post-contrast enhancement, oedema and mass effect can often be seen.[25,28]

Solitary fibrous tumour

Solitary fibrous tumours, previously known as haemangiopericytomas, are rare, highly vascular, dural-based tumours of mesenchymal origin. They have a peak in the

fourth to sixth decades of life, and typically arise from the musculoskeletal system, retroperitoneum, head, and neck.[30,31] When primary CNS solitary fibrous tumours occur, they have the unusual ability to metastasise through the blood–brain barrier into the systemic system. Lung and bone are common sites of metastases.[31] Furthermore, solitary fibrous tumours are notorious for their ability to recur locally or distantly in up to 50% of cases, despite repeated surgical excisions.[31] Given their extra-axial nature, they are commonly misinterpreted as meningiomas on imaging and are potential mimics of SDH. Prominent flow voids within the mass, indicating their highly vascular nature, as well as adjacent bony erosion, are some radiological signs that distinguish these types of tumours.[16,31]

Ischaemia

Hypoxic ischaemic injury

Hypoxic ischaemic injury (HII) occurs as a consequence of global hypoxaemia or hypoperfusion, often secondary to a cerebrovascular accident or acute myocardial infarction, and manifests neurologically as diffuse cerebral oedema. Although the finding of pseudo-subarachnoid haemorrhage has been reported widely in patients with HII, there have also been isolated reports of apparent high-density areas along the falx and the tentorium cerebelli mimicking SDH (Fig 6).[32] The pathophysiology for this "pseudo-SDH" appearance has not been specifically explained in the literature. The authors postulate that it may be similar to the pathophysiology of pseudo-subarachnoid haemorrhage: engorgement of the superficial veins (due to compromise of venous drainage from compression of the dural sinuses) and relative hypo-attenuation of the brain parenchyma results in seemingly high-density areas along the falx and tentorium on CT that mimic SDHs.[33,34]

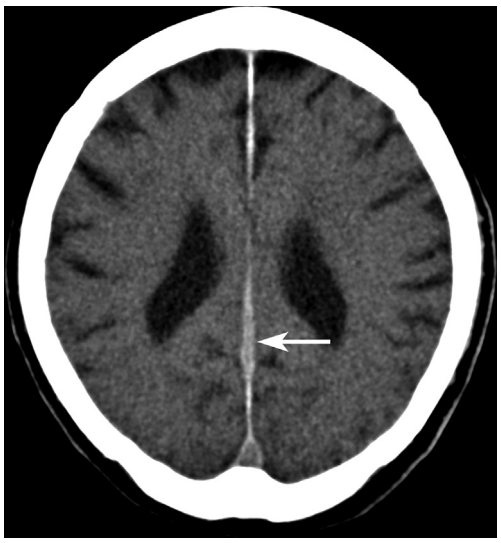

Figure 6 A CT head was performed in a 78-year-old man 3 days post-pulseless electrical activity (PEA) collapse with poor neurological recovery. Unenhanced axial CT images demonstrates abnormal thickening of the posterior interhemispheric falx, mimicking an acute SDH (white arrow). Note that there is diffuse cerebral oedema and loss of grey–white differentiation. The conglomeration of findings is from HII.

In distinction with isolated SDH, HII results in diffuse cerebral oedema with sulcal effacement. CT may show loss of grey–white differentiation and decreased bilateral basal ganglia attenuation. In severe cases, a "reversal sign" may be present whereby diffusely decreased density of the cerebral hemispheres, and relative increased density of the thalami, brainstem, and cerebellum is noted.[35,36]

Inflammation and infection

Hypertrophic pachymeningitis

Hypertrophic pachymeningitis is a rare form of diffuse inflammatory disease that causes thickening of the dura mater as well as the underlying and neighbouring leptomeninges.[37] It may be idiopathic in nature or may occur secondary to inflammatory or infective causes such as rheumatoid arthritis, syphilis, granulomatosis with polyangitis (Fig 7a,b), tuberculosis, IgG4-related disease (Fig 7c,d), and carcinoma.[38] Relevant clinical history and assessment of organ systems outside of the CNS is paramount in distinguishing this subdural mimic from a true SDH.

Hypertrophic pachymeningitis appears as thickened, nodular areas of dura, typically along the tentorium, tentorial ridge, falx, and brain stem.[37,39] The thickened dura can appear hyperdense on CT, mimicking SDH.[37] On MRI, the thickened dura is hypointense on T1-weighted and T2-weighted images. Marked enhancement is noted on post-contrast images, and associated leptomeningeal enhancement is common.[40]

Rosai–Dorfman disease

Rosai–Dorfman disease (RDD) is a benign systemic histio-proliferative disease, causing painless massive lymphadenopathy, fever, leukocytosis, elevated erythrocyte sedimentation rate (ESR), and hypergammaglobulinaemia.[41] It affects people of all ages, with a predilection for males in their first and second decade of life.[42] Although histiocytes in RDD often accumulate in the lymph nodes, several extranodal sites such as the skin, paranasal sinuses, nasal cavity, salivary glands, eyes, and adnexal structures have been implicated as well; in $<5\%$ of cases, it may affect the CNS meninges or brain and spinal cord parenchyma.[43] Its aetiology is still not wholly certain, with viral and autoimmune origins postulated in the literature.[42] In some cases, RDD may be a self-limiting condition not requiring treatment; if CNS involvement is noted, local mass effect may cause clinical symptoms requiring more aggressive measures such as surgery, radiation, and chemotherapy.[42]

On imaging, the most common CNS pattern is that of an extra-axial, well-circumscribed, dural-based mass, which is isodense or hyperdense on CT (Fig 7e).[42,44,45] On MRI, it is

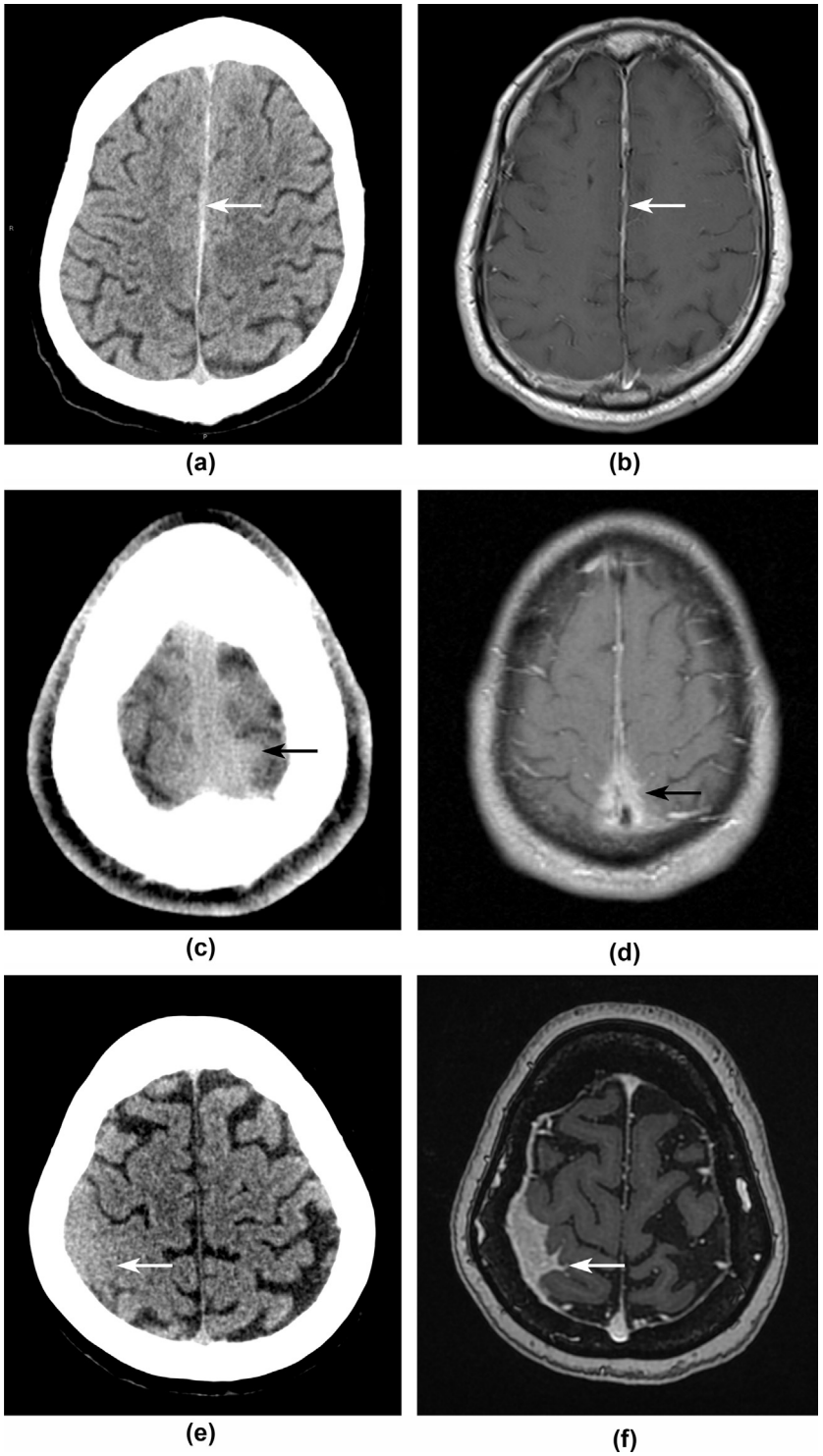

Figure 7 Inflammatory processes that mimic SDHs. Patient 1: a 47-year-old man with a history of granulomatosis with polyangiitis (GPA). (a) Unenhanced axial CT head image demonstrates hyperdense thickening of the falx cerebri (white arrow). (b) Post-contrast T1-weighted axial MRI image demonstrates diffuse enhancement of the interhemispheric falx (white arrow). The findings represent GPA-related pachymeningitis. Patient 2: a middle-aged man with history of multifocal sclerosis and retroperitoneal fibrosis presenting with headache. (c) Unenhanced axial CT head image demonstrates hyperdense thickening of the falx cerebri, extending posteriorly to surround the superior sagittal sinus (black arrow). (d) Post-contrast T1-weighted axial MRI image shows diffuse enhancement of the lesion (black arrow). The pachymeningeal thickening was related to IgG4-related meningeal involvement. Patient 3: a CT head was performed for a middle-aged patient. (e) Unenhanced axial CT head shows an extra-axial mass along the right parietal convexity (white arrow). Potential considerations included subdural haemorrhage and a neoplastic mass. Subsequent open biopsy showed RDD. (f) Note that on MRI, the enhancement extends into the leptomeninges (white arrow), which has been described with RDD and may be an important clue towards diagnosis.

isointense on T1-weighted images and isointense to hypointense on T2-weighted images (Fig 7f).[44] In contrast to SDH, accompanying leptomeningeal enhancement, central lesion enhancement, and massive lymphadenopathy may be seen.[43,44,46,47] Surrounding vasogenic oedema is often present.[44]

Empyema

Subdural empyemas are a neurosurgical emergency. Most evolve from sinusitis due to direct extension from an infected sinus and osteomyelitis, or haematogenic spread due to retrograde thrombophlebitis. Other causes include meningitis, otitis media, post-surgical complications, dental infections, previous head trauma, or bacteraemic seeding of a previous SDH.[21,48]

Empyemas appear as an extra-axial fluid collection, which is isodense or hypodense on CT (Fig 8a). They demonstrate peripheral rim enhancement secondary to granulation tissue formation as a result of chronic infection (Fig 8b). They are usually unilateral, but may occasionally be bilateral. Associated paranasal sinus or mastoid disease is frequently noted.[4,21,48] Decreased grey–white matter differentiation of the adjacent cerebral hemisphere secondary to cytotoxic oedema can be seen. On MRI, most, but not all, empyemas demonstrate restricted diffusion (Fig 8c).[49]

Traumatic and iatrogenic

Extra-dural haematoma

Extra-dural haematomas (EDH) occur most commonly as a result of laceration of the middle meningeal artery secondary to head trauma, and are often associated with temporal bone skull fractures.[4,50] The majority of EDHs (85–90%) are associated with a fracture of the calvarium.[4]

An acute EDH typically appears as a hyperdense biconvex extra-axial lesion on CT (Fig 9a), and does not have the crescentic tail associated with SDH.[50] In contradistinction to SDHs, EDHs do not cross suture lines (unless sutural diastasis or a fracture is present), yet can cross the falx cerebri and tentorium.[4]

Subdural hygroma

Subdural hygromas are an accumulation of CSF in the subdural space. They are thought to occur as a result of separation of the dura arachnoid interface after trauma, presenting as small subdural fluid collections as early as 24 hours after the onset of trauma.[51–54]

Pure subdural hygromas manifest as extra-axial collections with density and signal similar to CSF on both CT and MRI, respectively (Fig 9b,c); however, there have been reports noting interval development of increased density within on CT,[52,53] and some hyperintense signal on fluid-attenuated inversion recovery (FLAIR) MRI[4]; this is likely related to the CSF admixed with some traumatic haemorrhage, accounting for lack of complete adherence to CSF density and signal intensity on CT and MRI.[2] Hygromas are typically bilateral and most often located in the frontal or temporal convexities.[53] Similar to other subdural processes, cortical veins will be displaced deep and pasted along the margin of the displaced cortex; cortical veins should not traverse the fluid collections.[52]

Intracranial hypotension

Intracranial hypotension is defined as CSF pressure <6 cmH_2O during lumbar puncture,[55,56] with normal CSF pressure in healthy individuals being 10–20 cmH_2O.[57] Primary intracranial hypotension results from spontaneous CSF leaks, while secondary intracranial hypotension results usually from iatrogenic factors (e.g. lumbar puncture or surgery) or over-shunting due to diversion devices or trauma.[55,58]

According to the Monro–Kellie hypothesis, CSF leaks along the neuraxis lead to alterations in the equilibrium between the volumes of intracranial blood, CSF, and brain tissue. To compensate for the decrease in CSF volume levels,

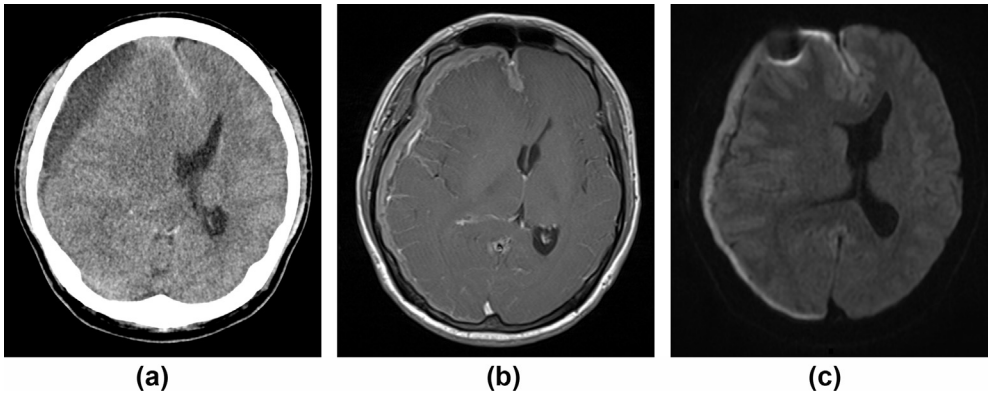

Figure 8 A 33-year-old man with advanced human immunodeficiency virus (HIV) disease and known cytomegalovirus (CMV) ventriculitis presenting with acute lethargy, vomiting, and headache. (a) Unenhanced axial CT head image shows an extra-axial hypodense fluid collection along the right cerebral convexity. (b) On the T1-weighted post-contrast axial MRI image, the lesion demonstrates peripheral rim enhancement. (c) Restricted diffusion is noted on diffusion-weighted imaging. This collection was drained and pus was noted at surgery. This was consistent with a subdural empyema.

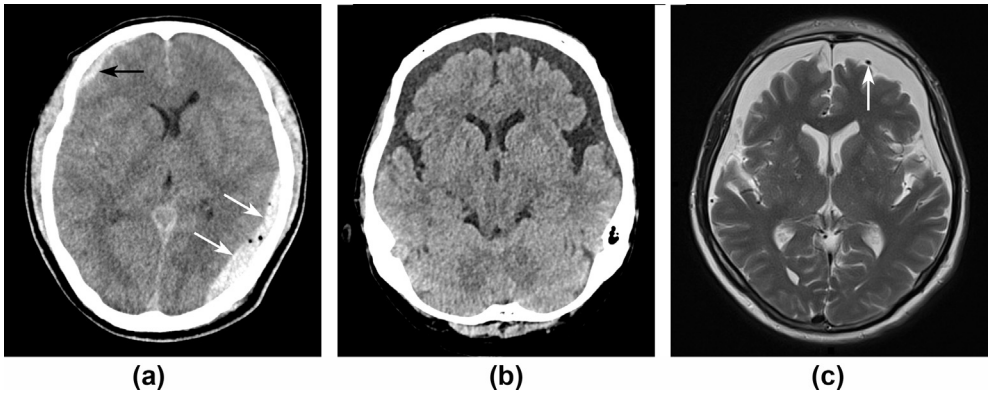

Figure 9 Traumatic processes that mimic SDHs. Patient 1: a 44-year-old man presenting to the emergency room after a fall from height. (a) Unenhanced axial CT head image demonstrates a crescent-shaped hyperdensity along the left cerebral convexity (white arrows). Note the presence of air pockets, which indicates the presence of a fracture. The findings represent an extra-dural haematoma. Note that there is also a true sliver of acute SDH along the frontal aspect of the right cerebral convexity (black arrow). Patient 2: a 59-year-old man presenting with headache. (b) Unenhanced axial CT head image demonstrates hypodense extra-axial collections overlying both frontal convexities. (c) On the T2 -weighted axial MRI image, these collections are noted to be the same signal intensity as CSF. Note the presence of a small vessel displaced and pasted along the left frontal cortex (white arrow). The findings represent subdural hygromas.

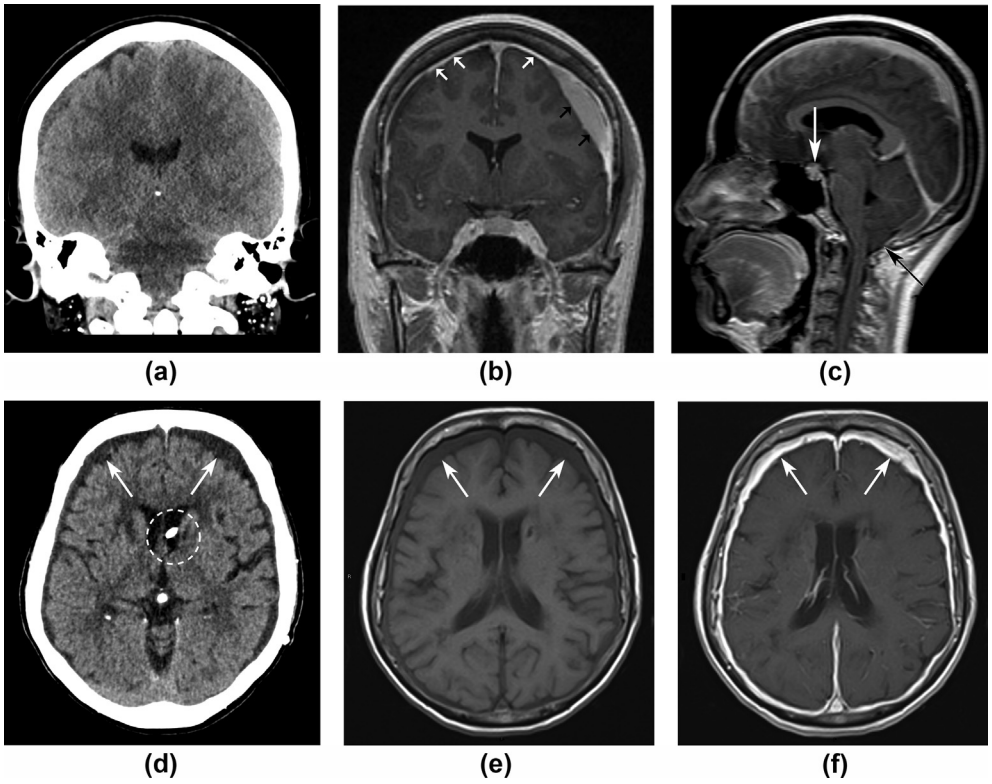

Figure 10 Iatrogenic conditions that mimic SDHs. Patient 1: a 55-year-old woman presenting with headache, nausea, and vomiting. (a) Unenhanced coronal CT head image demonstrates a hypodense collection along the right cerebral convexity, and a mixed density collection along the left cerebral convexity. (b,c) Coronal and sagittal T1-weighted post-contrast images show diffuse pachymeningeal thickening and enhancement (short white arrows), and a late subacute SDH along the left cerebral convexity (short black arrows). Cerebellar tonsillar herniation (black arrow) and engorgement of the pituitary gland (long white arrow) are also noted, confirming the diagnosis of intracranial hypotension. Patient 2: an 84-year-old woman had a follow-up CT head performed to assess for hydrocephalus after excision of an acoustic neuroma at the cerebellopontine angle, which required insertion of a ventriculo-peritoneal (VP) catheter. (d) Unenhanced axial and coronal CT brain images show bilateral expanded low-density extra-axial spaces mimicking chronic SDHs (white arrows). The tip of a VP shunt can be seen within the frontal horn of the left lateral ventricle (dotted white circle). (e,f) Axial pre and post-contrast T1-weighted axial MRI images demonstrate diffuse contrast enhancement of these extra-axial spaces (white arrows), in keeping with meningeal fibrosis.

Table 3
Common mimics of subdural haematomas (SDHs) and tips to distinguish them from true SDH.

Pathology of mimic	Post-contrast Enhancement	Key distinguishing factors
NORMAL ANATOMY and ARTEFACTS		
Prominent venous sinuses	Yes	• Location along the anterior rim of the middle cranial fossa (sphenoparietal venous sinus) • Hyperdense appearance may result, particularly if haematocrit levels are raised
Prominent cortical veins	Yes	• Careful inspection of adjacent image sections • Inspection of the pathology on orthogonal projections
Frontal lobes that extend into the middle cranial fossa	No	• Careful inspection of adjacent image sections • Presence of grey white differentiation
Cerebellar flocculus	No	
Beam hardening artefact	No	• Linear areas of streaky density arising from the dense object, not infrequently from bone
Motion artefact	No	• Blurring of adjacent brain and bone
Tumours		
Lymphoma	Yes (associated with lack of trauma history, persistence or growth on follow up imaging)	• Nodular/lobulate appearance of borders • Involvement of adjacent structures
Metastases		• Nodular/lobulate appearance of borders • Presence of adjacent bone metastases • Clinical history of systemic primary neoplasm • Concurrent SDH may be present
Meningioma		• Dural tail • Cleft sign • Hyperostosis of adjacent bone
Granulocytic sarcoma		• Clinical history of systemic leukaemia • Child or young teenager
Solitary fibrous tumour		• Prominent flow voids (due to increased vascularity) • Adjacent bone erosion
Ischaemic		
Hypoxic ischaemic injury	Yes	• Clinical history of hypoxaemia/hypoperfusion • Diffuse cerebral oedema • +/- presence of reversal sign
INFLAMMATION and INFECTION		
Hypertrophic pachymeningitis	Yes	• Thickened, nodular areas of dura • Associated leptomeningeal enhancement • Clinical history of associated systemic disorder
Rosai–Dorfman Disease	Yes	• Clinical history of massive lymphadenopathy • Possible leptomeningeal enhancement
Empyema	Yes (rim-enhancement)	• Presence of cytotoxic oedema in adjacent brain parenchyma • Associated paranasal sinus or mastoid disease • Restricted diffusion on DWI • Clinical stigmata of CNS infection
TRAUMA and IATROGENIC		
Epidural haematoma	No	• Biconvex extra-axial hyperdensity • History of trauma with calvarium fracture • Bounded by sutures unless sutural diastasis/fracture present
Subdural hygroma	No	• Extra-axial collection with a density and signal intensity similar to CSF
Intracranial hypotension	Yes	• Inferior displacement of the brain • Subdural fluid collections • Pachymeningeal thickening • Venous distention sign • Look for accompanying ventricular shunt • Concurrent SDH may be present
Post-shunt meningeal fibrosis	Yes	• Presence of a ventricular shunt • Presence of expanded low density extra-axial spaces on CT • Diffuse pachymeningeal enhancement after contrast medium administration

CNS, central nervous system; CSF, cerebrospinal fluid; CT, computed tomography.

there is subsequent dilatation of the dural sinuses, which can mimic SDH.[55,58]

Acute SDH has also been reported to simultaneously occur in intracranial hypotension, likely as a result of decreased CSF leading to decrease buoyant support on the brain and increased traction and rupture of bridging cortical veins.[59]

Intracranial hypotension can present with extensive pachymeningeal thickening, which can mimic a low-density SDH on CT (Fig 10a). The diffuse pachymeningeal thickening and enhancement is more readily appreciated on post-contrast MRI (Fig 10b). Concomitant true SDHs and subdural fluid collections are not uncommonly present.[55,60] Given the low intracranial pressure state, pituitary gland engorgement, cerebellar tonsillar herniation, effacement of prepontine and perichiasmatic cisterns and inferior displacement of the optic chiasm have also been described (Fig 10c).[55,60] The normally concave inferior surface of the transverse sinus can become convex in appearance, giving rise to the "venous distension sign".[58]

Post-shunt meningeal fibrosis

Fibrosis of the pachymeninges was a term that was written about in the radiological literature in the 1980s.[61] It appears that this phrase has fallen out of favour in recent years. According to descriptions of post-shunt meningeal fibrosis and secondary intracranial hypotension, it appears that these terms are equivalent, although to the authors' knowledge, this has not been explicitly stated in the literature. As the term implies, this refers to the development of meningeal fibrosis in patients with chronic ventricular shunting. It is not an uncommon entity, and on CT manifests as an expanded low-density extra-axial space, similar in appearance to CSF (Fig 10d), and therefore a potential mimic for chronic subdural haematomas.[62] On MRI, it appears hypointense on T1-weighted sequences and hyperintense on T2-weighted sequences, and demonstrates post-contrast enhancement (Fig 10e,f).[61] Indeed these extra-axial "collections" have been biopsied in the past, showing fibrosis of the meninges containing granulation tissue and collagen deposition.[61] The presence of a long-standing CSF shunt catheter will be the tip-off that post shunt meningeal fibrosis is present.

Conclusion

A wide range of normal and pathologic processes can mimic SDHs. Understanding the typical characteristics of a SDH and close inspection of the morphology of the subdural process and changes to the adjacent bone and brain may help in distinguishing between a true SDH from a SDH mimic (Table 3). Clinical history can also be paramount in this regard. There may be instances in which it may be challenging to distinguish between these entities. In such cases, a contrast-enhanced examination or MRI may ultimately be necessary for further characterisation.

Radiologists and clinicians alike should think twice upon encountering another "SDH" on an emergency room CT, as making the distinction between a SDH and its mimics is vital to appropriately directed clinical management.

Conflict of interest

The authors declare no conflict of interest.

Acknowledgements

The authors thank Insil Choi of the John Hopkins University School of Medicine, who contributed the illustration for Fig 1 in this manuscript, as well as Dr Andrew Makmur of the National University Hospital Singapore who contributed the case of RDD disease.

References

1. Catana D, Koziarz A, Cenic A, *et al*. Subdural hematoma mimickers: a systematic review. *World Neurosurg* 2016;**93**:73–80. https://doi.org/10.1016/j.wneu.2016.05.084.
2. Lindsay D, Small J. Subdural hemorrhage and posttraumatic hygroma. In: Small JE, Noujaim DL, Ginat DT, *et al*., editors. *Neuroradiology: spectrum and evolution of disease*. 1st edn. Philadelphia: Elsevier; 2018. p. 6–19.
3. Teale EA, Iliffe S, Young JB. Subdural haematoma in the elderly. *BMJ* 2014;**348**. https://doi.org/10.1136/bmj.g1682.
4. Stoffey RD, Nadgir R, Yousem D. Head trauma. In: Stoffey RD, Nadgir R, Yousem D, editors. *Neuroradiology: the requisites*. 4th edn. Philadelphia: Elsevier; 2017. p. 150–73.
5. Fobben ES, Grossman RI, Atlas SW, *et al*. MR characteristics of subdural hematomas and hygromas at 1.5 T. *AJNR Am J Neuroradiol* 1989 Sep;**153**(3):589–95.
6. Carroll JJ, Lavine SD, Meyers PM. Imaging of subdural hematomas. *Neurosurg Clin N Am* 2017 Apr;**28**(2):179–203. https://doi.org/10.1016/j.nec.2016.11.001.
7. Aring CD, Evans JP. Aberrant location of subdural hematoma. *Arch Neurol Psychiatry* 1940;**44**(6):1296–306. https://doi.org/10.1001/archneurpsyc.1940.02280120143014.
8. Hirakawa K, Hashizume K, Fuchinoue T, *et al*. Statistical analysis of chronic subdural hematoma in 309 adult cases. *Neurol Med Chir (Tokyo)* 1972;**12**:71–83.
9. Kawoosa NN, Bhat AR, Rashid B. Interhemispheric acute subdural hematomas. *Iran Red Crescent Med J* 2011;**13**(4):289–90.
10. Black DF, Rad AE, Gray LA, *et al*. Cerebral venous sinus density on noncontrast CT correlates with hematocrit. *AJNR Am J Neuroradiol* 2011 Aug;**32**(7):1354–7. https://doi.org/10.3174/ajnr.A2504. Epub 2011 May 12.
11. Kilic T, Akakin A. Anatomy of cerebral veins and sinuses. *Front Neurol Neurosci* 2008;**23**:4–15.
12. McKinney AM. Cerebellar flocculus pseudomass. In: *Atlas of normal imaging variations of the brain, skull, and craniocervical vasculature*. Cham: Springer; 2017. p. 13–8. https://doi.org/10.1007/978-3-319-39790-0_3.
13. Barrett JF, Keat N. Artifacts in CT: recognition and avoidance. *RadioGraphics* 2004 Nov-Dec;**24**(6):1679–91.
14. Tiftik N, Unlu K, Ayyildiz O, *et al*. Images in haematology. *Turk J Haematol* 2001;**18**(2):147.
15. Gocmen S, Gamsizkan M, Onguru O, *et al*. Primary dural lymphoma mimicking a subdural hematoma. *J Clin Neurosci* 2010 Mar;**17**(3):380–2. https://doi.org/10.1016/j.jocn.2009.02.014. Epub 2010 Jan 15.
16. Smith AB, Horkanyne-Szakaly I, Schroeder JW, *et al*. From the Radiologic Pathology archives: mass lesions of the dura: beyond meningioma—radiologic–pathologic correlation. *RadioGraphics* 2014 Mar-Apr;**34**(2):295–312. https://doi.org/10.1148/rg.342130075.
17. Iwamoto FM, Abrey LE. Primary dural lymphomas: a review. *Neurosurg Focus* 2006 Nov 15;**21**(5):E5.

18. Chourmouzi D. Dural lesions mimicking meningiomas: a pictorial essay. *World J Radiol* 2012 Mar 28;**4**(3):75–82. https://doi.org/10.4329/wjr.v4.i3.75.
19. Haldorsen IS, Espeland A, Larsson EM. Central nervous system lymphoma: characteristic findings on traditional and advanced imaging. *Am J Neuroradiol* 2011 Jun-Jul;**32**(6):984–92. https://doi.org/10.3174/ajnr.A2171. Epub 2010 Jul 8.
20. Laigle-Donadey F, Taillibert S, Mokhtari K, *et al*. Dural metastases. *J Neuro oncol* 2005 Oct;**75**(1):57–61.
21. de Beer MH, van Gils AP, Koppen H. Mimics of subacute subdural hematoma in the ED. *Am J Emerg Med* 2013;**31**:1–3. https://doi.org/10.1016/j.ajem.2012.10.019.
22. Nzokou A, Magro E, Guilbert F, *et al*. Subdural metastasis of prostate cancer. *J Neurol Surg Rep* 2015;**76**(1):e123–7. https://doi.org/10.1055/s-0035-1549224.
23. Starr CJ, Cha S. Meningioma mimics: five key imaging features to differentiate them from meningiomas. *Clin Radiol* 2017 Sep;**72**(9):722–8. https://doi.org/10.1016/j.crad.2017.05.002. Epub 2017 May 26.
24. Stoffey RD, Nadgir R, Yousem D. Neoplasms of the brain. In: Stoffey RD, Nadgir R, Yousem D, editors. *Neuroradiology: the requisites*. 4th edn. Philadelphia: Elsevier; 2017. p. 40–86. https://doi.org/10.2214/AJR.10.6189.
25. Mallory GM, Van Gompel JJ, Rabinstein AA, *et al*. Wolf in sheep's clothing: acute chloroma disguised as a subdural hematoma. *Neurocrit Care* 2012 Feb;**16**(1):148–50. https://doi.org/10.1007/s12028-011-9631-7.
26. Wang HQ, Li J. Clinicopathological features of myeloid sarcoma: report of 39 cases and literature review. *Pathol Res Pract* 2016 Sep;**212**(9):817–24. https://doi.org/10.1016/j.prp.2016.06.014. Epub 2016 Jul 20.
27. Noh BW, Park S-W, Chun J-E, *et al*. Granulocytic sarcoma in the head and neck: CT and MRI findings. *Clin Exp Otorhinolaryngol* 2009 Jun;**2**(2):66–71. https://doi.org/10.3342/ceo.2009.2.2.66. Epub 2009 Jun 27.
28. Guermazi A, Feger C, Rousselot P, *et al*. Granulocytic sarcoma (chloroma). *AJR Am J Roentgenol* 2002;**178**(2):319–25. https://doi.org/10.2214/ajr.178.2.1780319.
29. Singh A, Kumar P, Chandrashekhara SH, *et al*. Unravelling chloroma: review of imaging findings. *Br J Radiol* 2017;**90**(1075):20160710. https://doi.org/10.1259/bjr.20160710.
30. Melone AG, D'Elia A, Santoro F, *et al*. Intracranial hemangiopericytoma — our experience in 30 years: a series of 43 cases and review of the literature. *World Neurosurg* 2014 Mar-Apr;**81**(3–4):556–62. https://doi.org/10.1016/j.wneu.2013.11.009. Epub 2013 Nov 13.
31. Ravenel JG, Goodman PC. Late pulmonary metastases from hemangiopericytoma of the mandible: unusual findings on CT and MRI. *AJR Am J Roentgenol* 2001 Jul;**177**(1):244–5.
32. Spiegel SM, Fox AJ, Vinuela F, *et al*. Increased density of tentorium and falx: a false positive CT sign of subarachnoid hemorrhage. *Can Assoc Radiol J* 1986 Dec;**37**(4):243–7.
33. Yuzawa H, Higano S, Mugikura S, *et al*. Pseudo-subarachnoid hemorrhage found in patients with postresuscitation encephalopathy: characteristics of CT findings and clinical importance. *AJNR Am J Neuroradiol* 2008 Sep;**29**(8):1544–9. https://doi.org/10.3174/ajnr.A1167. Epub 2008 Jun 12.
34. Rabinstein AA, Pittock SJ, Miller GM, *et al*. Pseudosubarachnoid haemorrhage in subdural haematoma. *J Neurol Neurosurg Psychiatry* 2003 Aug;**74**(8):1131–2.
35. Huang BY, Castillo M. Hypoxic–ischaemic brain injury: imaging findings from birth to adulthood. *RadioGraphics* 2008;**28**(2):417–39. https://doi.org/10.1148/rg.282075066.
36. Shroff M, Chavhan G. Twenty classic signs in neuroradiology: a pictorial essay. *Indian J Radiol Imaging* 2009 Apr-Jun;**19**(2):135–45. https://doi.org/10.4103/0971-3026.50835.
37. Karthik SN, Bhanu K, Velayutham S, *et al*. Hypertrophic pachymeningitis. *Ann Indian Acad Neurol* 2011;**14**(3):203–4. https://doi.org/10.4103/0972-2327.85896.
38. Kupersmith MJ, Martin V, Heller G, *et al*. Idiopathic hypertrophic pachymeningitis. *Neurology* 2004;**62**(5):686–94. https://doi.org/10.1212/01.WNL.0000113748.53023.B7.
39. Martin N, Masson C, Henin D, *et al*. Hypertrophic cranial pachymeningitis: assessment with CT and MRI 1989 May-Jun;**10**(3):477–84.
40. Friedman DP, Flanders AE. Enhanced MRI of hypertrophic pachymeningitis. *AJR Am J Roentgenol* 1997;**169**(5):1425–8. https://doi.org/10.2214/ajr.169.5.9353473.
41. Kushwaha R, Ahluwalia C, Sipayya V. Diagnosis of sinus histiocytosis with massive lymphadenopathy (Rosai–Dorfman disease) by fine needle aspiration cytology. *J Cytol* 2009;**26**(2):83–5. https://doi.org/10.4103/0970-9371.55229.
42. Sandoval-Sus JD, Sandoval-Leon AC, Chapman JR, *et al*. Rosai–Dorfman disease of the central nervous system: report of 6 cases and review of the literature. *Medicine (Baltimore)* 2014;**93**(3):165–75. https://doi.org/10.1097/MD.0000000000000030.
43. Kumar KK, Menon G, Nair S, *et al*. Rosai–Dorfman disease mimicking chronic subdural hematoma. *J Clin Neurosci* 2008 Nov;**15**(11):1293–5. https://doi.org/10.1016/j.jocn.2007.09.010. Epub 2008 Sep 27.
44. Zhu H, Qiu LH, Dou YF, *et al*. Imaging characteristics of Rosai–Dorfman disease in the central nervous system. *Eur J Radiol* 2012 Jun;**81**(6):1265–72. https://doi.org/10.1016/j.ejrad.2011.03.006. Epub 2011 Mar 25.
45. Kattner KA, Stroink AR, Roth TC, *et al*. Rosai–Dorfman disease mimicking parasagittal meningioma: case presentation and review of literature. *Surg Neurol* 2000 May;**53**(5):452–7. discussion 457.
46. Mahzoni P, Zavareh MHT, Bagheri M, *et al*. Intracranial rosai–dorfman disease. *J Res Med Sci* 2012;**17**(3):304–7.
47. Symss NP, Cugati G, Vasudevan MC, *et al*. Intracranial Rosai–Dorfman disease: report of three cases and literature review. *Asian J Neurosurg* 2010;**5**(2):19–30.
48. Sadhu VK, Handel SF, Pinto RS, *et al*. Neuroradiologic diagnosis of subdural empyema and CT limitations. *Am J Neuroradiol* 1980 Jan-Feb;**1**(1):39–44.
49. Chen R. Subdural empyema. In: Abujudeh HH, editor. *Emergency radiology cases*. 1st edn. New York: Oxford University Press; 2014. p. 194.
50. Su IC, Wang KC, Huang SH, *et al*. Differential CT features of acute lentiform subdural hematoma and epidural hematoma. *Clin Neurol Neurosurg* 2010 Sep;**112**(7):552–6. https://doi.org/10.1016/j.clineuro.2010.03.001. Epub 2010 May 18.
51. Deltour P, Lemmerling M, Bauters W, *et al*. Posttraumatic subdural hygroma: CT findings and differential diagnosis. *JBR-BTR* 1999 Aug;**82**(4):155–6.
52. McCluney KW, Yeakley JW, Fenstermacher MJ, *et al*. Subdural hygroma versus atrophy on MR brain scans: "the cortical vein sign. *AJNR Am J Neuroradiol* 1992 Sep-Oct;**13**(5):1335–9.
53. Kabir SM, Jennings SJ, Makris D. Posterior fossa subdural hygroma with supratentorial chronic subdural haematoma. *Br J Neurosurg* 2004 Jun;**18**(3):297–300.
54. Zanini MA, De Lima Resende LA, De Souza Faleiros AT, *et al*. Traumatic subdural hygromas: proposed pathogenesis based classification. *J Trauma* 2008 Mar;**64**(3):705–13. https://doi.org/10.1097/TA.0b013e3180485cfc.
55. Paldino M, Mogilner AY, Tenner MS. Intracranial hypotension syndrome: a comprehensive review. *Neurosurg Focus* 2003 Dec 15;**15**(6):ECP2.
56. Kranz PG, Tanpitukpongse TP, Choudhury KR, *et al*. How common is normal cerebrospinal fluid pressure in spontaneous intracranial hypotension? *Cephalalgia* 2015;**36**(13):1209–17. https://doi.org/10.1177/0333102415623071.
57. Wright BLC, Lai JTF, Sinclair AJ. Cerebrospinal fluid and lumbar puncture: a practical review. *J Neurol* 2012 Aug;**259**(8):1530–45. https://doi.org/10.1007/s00415-012-6413-x. Epub 2012 Jan 26.
58. Farb RI, Forghani R, Lee SK, *et al*. The venous distension sign: a diagnostic sign of intracranial hypotension at MRI of the brain. *Am J Neuroradiol* 2007 Sep;**28**(8):1489–93.
59. Jacobs MB, Wasserstein PH. Spontaneous intracranial hypotension. An uncommon and underrecognized cause of headache. *West J Med* 1991;**155**(2):178–80.
60. Pattichis A (Andreas), Slee M. CSF hypotension: a review of its manifestations, investigation and management. *J Clin Neurosci* 2016;**34**:39–43. https://doi.org/10.1016/j.jocn.2016.07.002.
61. Destian S, Heier LA, Zimmerman RD, *et al*. Differentiation between meningeal fibrosis and chronic subdural hematoma after ventricular shunting: value of enhanced CT and MR scans. *AJNR Am J Neuroradiol* 1989 Sep-Oct;**10**(5):1021–6.
62. Castillo M. Disorders of cerebral spinal fluid flow. In: *The core curriculum: neuroradiology*. Philadelphia: Lippincott Williams and Wilkins; 2002. p. 126.
63. Parizel PM, Makkat S, Van Miert E, *et al*. Intracranial hemorrhage: principles of CT and MRI interpretation. *Eur Radiol* 2001;**11**(9):1770–83.